Materials Transactions, Vol. 53, No. 10 (2012) pp. 1716 to 1720

Synthesis of Ni Carbide Nanoparticles with Ni_3C-Type Structure in Polyol Solution Containing Dispersant

Shun Fujieda[1,*], Kozo Shinoda[1], Shigeru Suzuki[1] and Balachandran Jeyadevan[2]

[1]*Institute of Multidisciplinary Research for Advanced Materials, Tohoku University, Sendai 980-8577, Japan*
[2]*Department of Materials Science, The University of Shiga Prefecture, Hikone 522-8533, Japan*

Nanoparticles of Ni carbide of about 50 nm in diameter were synthesized by the reduction of Ni salt in a polyol solution in the presence of polyvinylpyrrolidone (PVP). It was found that the aggregation of nanoparticles was suppressed when PVP was added to the polyol solution during synthesis. Diffraction peaks of the fcc and hexagonal structures were observed for the specimen synthesized without PVP. On the other hand, no peaks assigned to the fcc structure and no spontaneous magnetization were observed for the specimen synthesized with 50 g/L PVP, although pure bulk Ni are fcc structure and ferromagnetic at room temperature. Additionally, small peaks were observed in the X-ray diffraction pattern at $2\theta = 26.2$, 35.7 and 47.8°, originated not from the impurity phase but from the hexagonal phase. The specimen synthesized with 50 g/L PVP was fundamentally identified as Ni carbide with a Ni_3C-type structure, as small peaks mentioned above were assigned to super-lattice peaks. The structure parameters of the Ni carbide were refined by Rietveld analysis. It is concluded that the formation of the Ni carbide nanoparticles with Ni_3C-type structure in the polyol solution is enhanced by the addition of PVP. [doi:10.2320/matertrans.M2012160]

(Received May 1, 2012; Accepted July 17, 2012; Published September 5, 2012)

Keywords: *nickel carbide, polyol, polyvinylpyrrolidone*

1. Introduction

Various types of nanoparticles have attached much attention due to their possible application in the field of nanotechnology. Several studies have been made on the synthesis of carbide nanoparticles such as SiC, TiC, VC, Fe_3C, ZrC, NbC, HfC and TaC as well as metallic nanoparticles,[1–5] because these are promising for use as hard materials, catalysts and wide-band gap semiconductor materials. A synthesis method of carbide nanoparticles should be examined extensively because of their high potential.

The synthesis of Ni nanoparticles has been examined significantly.[6–23] Results have shown that synthesized nanoparticles contain a hexagonal phase in several investigations, while a bulk Ni metal has an fcc structure. In addition, the saturation magnetization of hexagonal phase has been reported to be much smaller than that of bulk Ni metal.[7–17,20,23] The hexagonal phase has been characterized as Ni carbide with a Ni_3C-type structure by some investigations using X-ray diffraction,[11,14,16,19,21,23] high-resolution transmission electron microscopy[14,20,22,23] and hard X-ray photoelectron spectroscopy.[11,12] However, the hexagonal phase has been identified as metallic Ni by several investigations.[8–10,13,15] In other words, it is still controversial as to whether the hexagonal phase is Ni carbide or metallic Ni in many investigations because the X-ray diffraction pattern in the International Center for Diffraction Data (ICDD) database of the former is very similar to that of the latter.[12,17] It is required to establish the synthesis condition of hexagonal phase and to characterize it in detail.

To obtain the hexagonal phase, we focused on precipitated particles synthesized by the reduction of Ni salt in a polyol solution. It has been reported that the volume fraction of the hexagonal and fcc phases in precipitated particles can be controlled by adjusting the reaction conditions in Ni salt-polyol system.[7] For example, the volume fraction of the hexagonal phase in precipitated particles increases with decreasing Ni salt concentration.[7] Moreover, the volume fraction of the hexagonal phase in precipitated particles obtained at a relatively high reaction temperature is more than that obtained at a relatively low reaction temperature. It has been suggested that the volume fraction of the hexagonal and fcc phases is influenced by the precipitated particle size in the polyol solution[7,9] because the precipitated particle size becomes smaller with decreasing the Ni salt concentration and with increasing reaction temperature.

In this study, the control of the precipitated particle size in the polyol solution was examined under the constant values of the Ni salt concentration and the reaction temperature by using different amounts of dispersant. According to the crystal structure data of thin Ni carbide film investigated by electron diffraction,[24,25] small super-lattice peaks are expected in the X-ray diffraction pattern of Ni carbide nanoparticles with a Ni_3C-type structure, although such peaks are not indicated in the X-ray diffraction pattern in the ICDD database. The X-ray diffraction pattern of the hexagonal phase synthesized in the polyol solution was characterized in detail.

2. Experiment

The specimens were synthesized in 100 ml of tetraethylene glycol solution containing 0.005 mol/L of Ni acetate tetrahydrate. Polyvinylpyrrolidone (PVP) was added to the solution as a dispersant. The reaction temperature and duration were 563 K and one hour, respectively. The precipitated particles were separated from the solution by centrifugation and washed in ethanol. The particle morphology and crystal structure of specimens were characterized by scanning electron microscopy and X-ray diffractometry with Cu-$K\alpha$ radiation, respectively. The X-ray diffraction data were collected in the 2θ region from 20 to 120° with a

*Corresponding author, E-mail: fujieda@tagne.tohoku.ac.jp

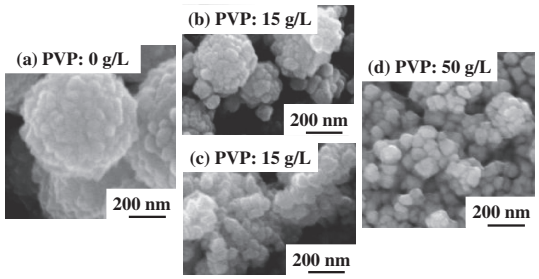

Fig. 1 SEM images of specimens synthesized with the different amounts of PVP: (a) 0, (b) and (c) 15, (d) 50 g/L.

step interval of 0.04°. The diffraction patterns were analyzed by a Rietvelt analysis program. Magnetic measurements were made with a superconducting quantum interference device (SQUID) magnetometer and a vibration sample magnetometer (VSM).

3. Results and Discussion

Figure 1 shows SEM images for specimens synthesized with different amounts of PVP. The specimen synthesized without PVP had aggregated particles more than 600 nm in diameter. Though aggregated particles were observed for the specimen synthesized with 15 g/L PVP, as shown in Fig. 1(b), their diameter is smaller than that for the specimen synthesized without PVP in Fig. 1(a). In addition, a part of the specimens consists of dispersed nanoparticles of about 50 nm in diameter, as seen in Fig. 1(c). Therefore, aggregation is suppressed by the addition of PVP. The dispersed nanoparticles of about 50 nm in diameter are mainly obtained by the addition of 50 g/L PVP, as shown in Fig. 1(d).

The X-ray diffraction patterns for the specimens synthesized with different amounts of PVP and the enlarged version of the same in the 2θ range between 25 and 55° are presented in Figs. 2(a) and 2(b), respectively. The short black bars in Fig. 2(a) indicate the X-ray diffraction patterns for the Ni_3C (No. 06-0697), the metallic Ni with hexagonal (No. 45-1027) and fcc (No. 04-0850) structures in the ICDD database. The diffraction peaks of the fcc and hexagonal phases are observed for the specimen synthesized without PVP. The peak intensities of the fcc phase are decreased with increasing amounts of PVP. As a result, no peaks assigned to the fcc structure are observed for the specimen synthesized with more than 15 g/L PVP, as shown in Fig. 2(b). Accordingly, the volume fraction of the fcc phase is decreased by the addition of PVP.

It is well known that metallic Ni with the fcc structure is ferromagnetic and possesses a saturation magnetization of about 55 emu/g at room temperature. On the other hand, the hexagonal phase synthesized in the polyol solution has been characterized as non-magnetic because the saturation magnetization becomes lower as the volume fraction of the hexagonal phase increases with decreasing Ni salt concentration.[7] Since the saturation magnetization for the fcc phase is much larger than that for the hexagonal phase, the magnetization measurement is meaningful to examine the influence of PVP on the volume fraction of the fcc phase in more detail. Figure 3 presents the magnetization curves at

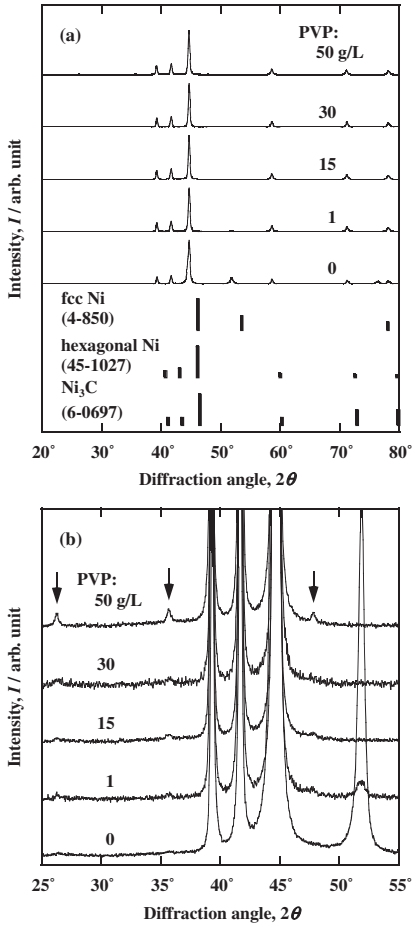

Fig. 2 (a) X-ray diffraction patterns for specimens synthesized by using the different amounts of PVP. The black short bars indicate the X-ray diffraction patterns for the Ni_3C (No. 06-0697), metallic Ni with hexagonal (No. 45-1027) and fcc (No. 04-0850) structures in the International Center for Diffraction Data (ICDD) database. (b) X-ray diffraction patterns enlarged in the 2θ range between 25 and 55°.

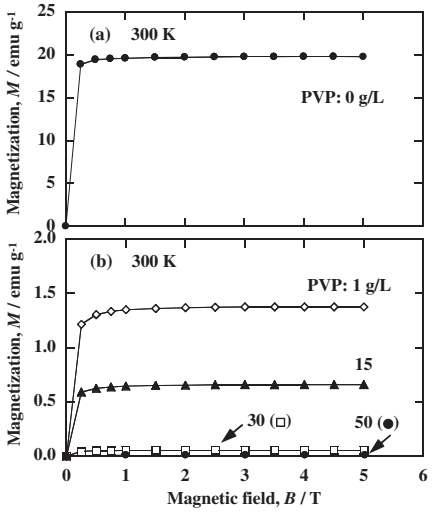

Fig. 3 Magnetization curves at 300 K for specimens synthesized with the different amounts of PVP.

300 K. The saturation magnetization decreases with increasing amounts of PVP. The saturation magnetization for the specimen synthesized with 30 g/L PVP is smaller than that

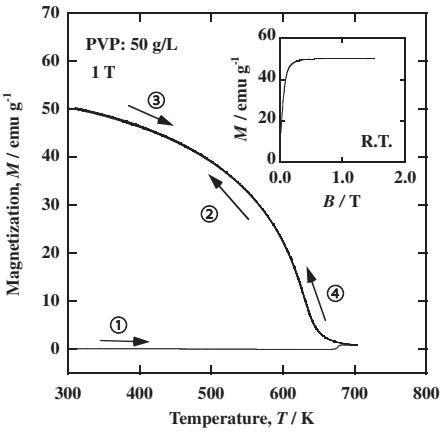

Fig. 4 Thermomagnetization curves in a magnetic field of 1 T for the specimen synthesized by using 50 g/L PVP. The heating and cooling processes are indicated by the arrows. The assigned numbers are the measurement sequence. The inset shows the magnetization curve at room temperature after thermomagnetization measurements.

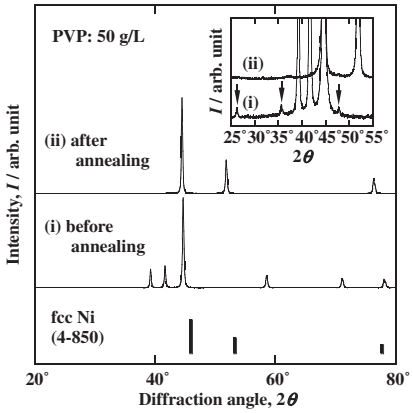

Fig. 5 X-ray diffraction patterns for the specimen synthesized by using 50 g/L PVP before and after annealing at 723 K. The short black bars indicate the X-ray diffraction patterns for metallic Ni with the fcc (No. 04-0850) in the International Center for Diffraction Data (ICDD) database.

for the specimen synthesized with 15 g/L PVP. In addition, no spontaneous magnetization is observed for the specimen synthesized with 50 g/L PVP. These results indicate that the specimens synthesized with 15 and 30 g/L PVP contain small fraction of the fcc phase, though the diffraction peaks corresponding to the fcc phase are not observed for the specimen synthesized with more than 15 g/L PVP in Fig. 2. The fcc phase almost disappears by the addition of 50 g/L PVP. However, the specimen synthesized with 50 g/L PVP is not identified as Ni carbide with a Ni_3C-type structure nor metallic Ni with a hexagonal structure by the ICDD database because small peaks were observed at $2\theta = 26.2$, 35.7 and 47.8° in the diffraction pattern, as indicated by arrows in Fig. 2(b). These peaks were not assigned as any Ni oxides.

Previously, it has been reported that the hexagonal phase synthesized in the polyol solution changes to the fcc phase by annealing.[7] Hence a significant change of magnetization due to the crystallographic transition is expected by annealing for the specimen synthesized with PVP. To appear the crystallographic transition temperature, Fig. 4 presents the thermomagnetization curves in a magnetic field of 1 T for the specimen synthesized with 50 g/L PVP. The heating and cooling processes are indicated by the arrows. The assigned numbers are the measurement sequence. The inset shows the magnetization curve at room temperature after thermomagnetization measurements. As shown in thermomagnetization curve ①, the magnetization exhibits an increase at 675 K. Thermomagnetization curve ② exhibits an increase of magnetization with decreasing temperature. Similar ferromagnetic behavior is observed in thermomagnetization curves ③ and ④. From thermomagnetization curves ②, ③ and ④, the Curie temperature T_C is estimated to be about 630 K, which corresponds to $T_C = 630$ K of the metallic Ni with fcc structure. In addition, the saturation magnetization at room temperature after thermomagnetization measurement is about 55 emu/g, which is also very close to that for metallic Ni with an fcc structure. Therefore, the crystallographic transition from hexagonal to fcc in the specimen synthesized with 50 g/L PVP occurs around 675 K.

To investigate the relationship between the diffraction peaks indicated by the arrows in Fig. 2(b) and the hexagonal phase, Fig. 5 presents the X-ray diffraction patterns for the specimen synthesized with 50 g/L PVP before and after annealing at 723 K. In addition, the inset shows the diffraction patterns enlarged in the 2θ range between 25 and 55°. The diffraction peaks of the hexagonal phase disappear after annealing at 723 K. In addition, the diffraction peaks at $2\theta = 26.2$, 35.7 and 47.8° also disappear after annealing at 723 K, as shown in the inset in Fig. 5. Thus, the specimen annealed at 723 K is identified as the fcc single phase. It is suggested that the diffraction peaks indicated by arrows in Fig. 2(a) and the inset in Fig. 5 originate not from the impurity phase but from the hexagonal phase.

Thin Ni carbide film with the Ni_3C-type structure has been made by annealing of thin Ni film with the fcc structure in a CO gas stream, and its crystal structure has been analyzed by electron diffraction.[24,25] It has been proposed that the crystal structure of Ni_3C belongs to the space group $R\bar{3}c$ and that Ni atoms occupy the 18*e* position with the fractional coordinates of $(x, 0, 1/4)$ and that carbon atoms occupy the 6*b* position with the fractional coordinates of $(0, 0, 0)$.[24,25] In this structure, the Ni atoms form a hexagonal lattice and the carbon atoms occupy one-third of the octahedral interstitial site of the Ni hexagonal lattice. Super-lattice peaks have been observed for Ni carbide film with the Ni_3C-type structure by the electron diffraction.[24,25] In addition, such peaks has been observed recently in the X-ray diffraction pattern of Ni carbide nanoparticles with the Ni_3C-type structure precipitated in the solution,[23] although these are not indicated in the X-ray diffraction pattern in the ICDD database.[12,17] Thus the X-ray powder diffraction pattern for the specimen synthesized with 50 g/L PVP was analyzed by Rietveld analysis by using the structure model of Ni_3C mentioned above. The refined results of the Rietveld analysis are shown in Fig. 6. In the figure, the cross and the solid line stand for the observed and calculated patterns, respectively. The dotted curve at the bottom denotes the difference between the observed and calculated data. The carbon atom occupation was treated as a free fitting parameter. From the difference

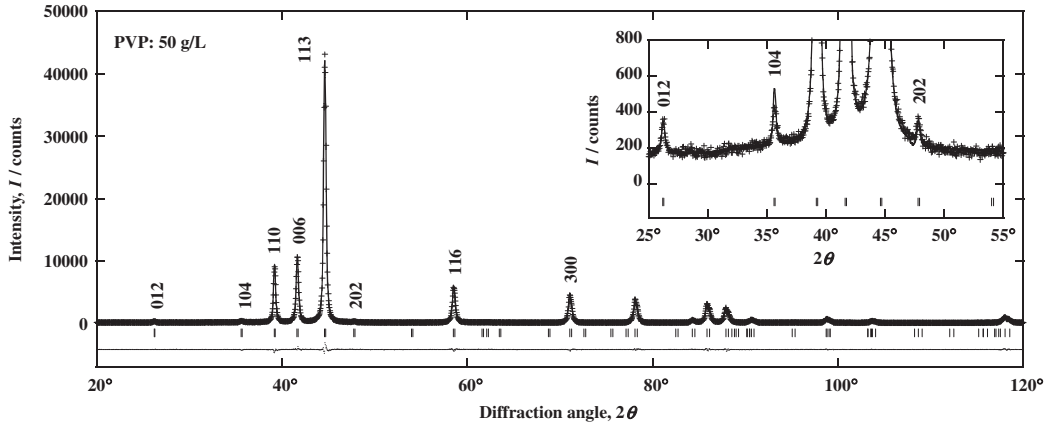

Fig. 6 X-ray diffraction pattern of the specimen synthesized with 50 g/L PVP. The cross and solid line stand for the observed and calculated patterns, respectively. The vertical short bars below the pattern indicate the calculated Bragg diffraction pattern of the Ni_3C structure. The difference between the observed and calculated data is shown at the bottom by the dotted curve. Inset shows the X-ray diffraction patterns enlarged in the 2θ range between 25 and 55°.

Table 1 Crystal structure parameters of the specimen synthesized using 50 g/L PVP: the lattice constants a, b, c, the frictional coordinates x, y, z, the occupancy g and the isotropic displacement parameter B, together with the reliability factors R_{wp} and R_B and the goodness of fit indicator S.

Lattice constant $a = b = 4.5889(1)$ Å, $c = 12.9895(2)$ Å
$R_{wp} = 5.72$, $R_B = 1.29$, $S = 1.33$

Atom	Site	x	y	z	g	B (Å^2)
C	6*b*	0.0	0.0	0.0	0.90(1)	0.51(2)
Ni	18*e*	0.3293(2)	0.0	0.25	1.00	0.75(1)

between the observed and calculated patterns, the reliability factors R_{wp} and R_B as well as the goodness of fit indicator S were evaluated. The inset shows the refined results enlarged in the 2θ range between 25 and 55°. Excellent agreement is obtained by using the structure parameters given in Table 1. Note that the small diffraction peaks at $2\theta = 26.2$, 35.7 and 47.8° are also assigned to 012, 104 and 202 super-lattice peaks of the Ni carbide with the Ni_3C-type structure. Accordingly, the specimen synthesized with 50 g/L PVP are mainly composed not of metallic Ni with the hexagonal structure but of Ni carbide with the Ni_3C-type structure.

Finally, we discuss the influence of PVP on the formation of Ni carbide with the Ni_3C-type hexagonal structure. For the specimen synthesized without PVP, the values of a and c were evaluated to be about 4.582 and 12.994 Å, respectively, from the data shown in Fig. 2(a). These values are very close to those for the specimen synthesized with 50 g/L PVP, indicating that the carbon content in the hexagonal phase for the latter is almost the same as that for the former. In other words, the hexagonal phase in the specimen synthesized without PVP is also mainly composed of Ni carbide with the Ni_3C-type structure. Consequently, the volume fraction of Ni carbide is fundamentally influenced by the addition of PVP. The surface area of the specimen becomes larger with increasing amounts of PVP, as can be understood from Fig. 1. Such change of particle morphology accelerates the supply of carbon from the surface. Therefore, it can be concluded that the enhancement of Ni carbide formation due to the addition of PVP is closely related to the suppression of aggregation.

4. Conclusion

Nanoparticles of about 50 nm in diameter were obtained by the reduction of Ni salt in a polyol solution with 50 g/L polyvinylpyrrolidone (PVP), though the specimen synthesized without PVP consisted of aggregated particles about 600 nm in diameter. Diffraction peaks of the hexagonal and fcc structures were observed for the specimen synthesized without PVP. No peaks assigned to the fcc structure and no spontaneous magnetization were observed for the specimen synthesized with 50 g/L PVP. Additionally, small peaks were observed in the X-ray diffraction pattern at $2\theta = 26.2$, 35.7 and 47.8°, which originated not from the impurity phase but from the hexagonal phase. The hexagonal phase was identified as Ni carbide with the Ni_3C-type structure by the Rietveld analysis of X-ray diffraction pattern, although these peaks were not indicated in the International Center for Diffraction Data (ICDD) database. Consequently, the formation of Ni carbide nanoparticles with the Ni_3C-type structure in the polyol solution was enhanced by the addition of PVP.

Acknowledgements

The present work was supported by a Grant-in-Aid for Young Scientists (B) (No. 23760620) from Japan Society for Promotion of Science. The authors thank Mr. K. Kuboniwa for his experimental support.

REFERENCES

1) A. Fukunaga, S. Chu and M. E. McHenry: J. Mater. Res. **13** (1998) 2465–2471.
2) Y. H. Chang, C. W. Chiu, Y. C. Chen, C. C. Wu, C. P. Tsai, J. L. Wang and H. T. Chiu: J. Mater. Chem. **12** (2002) 2189–2191.
3) J. A. Nelson and M. J. Wagner: Chem. Mater. **14** (2002) 4460–4463.
4) Z. Liu, L. Ci, N. Y. Jin-Phillipp and M. Rühle: J. Phys. Chem. C **111** (2007) 12517–12521.
5) D. E. Grove, U. Gupta and A. W. Castleman, Jr.: Langmuir **26** (2010)

16517–16521.
6) G. Carturan, G. Cocco, S. Enzo, R. Ganzerla and M. Lenarda: Mater. Lett. **7** (1988) 47–50.
7) C. N. Chinnasamy, B. Jeyadevan, K. Shinoda, K. Tohji, A. Narayanasamy, K. Sato and S. Hisano: J. Appl. Phys. **97** (2005) 10J309 1–3.
8) Y. Mi, D. Yuan, Y. Liu, J. Zhang and Y. Xiao: Mater. Chem. Phys. **89** (2005) 359–361.
9) V. Tzitzios, G. Basina, M. Gjoka, V. Alexandrakis, V. Georgakilas, D. Niarchos, N. Boukos and D. Petridis: Nanotechnology **17** (2006) 3750–3755.
10) Y. T. Jeon, J. Y. Moon, G. H. Lee, J. Park and Y. Chang: J. Phys. Chem. B **110** (2006) 1187–1191.
11) Y. Leng, H. Shao, Y. Wang, M. Suzuki and X. Li: J. Nanosci. Nanotechnol. **6** (2006) 221–226.
12) Y. Goto, K. Taniguchi, T. Omata, S. Otsuka-Yao-Matsuo, N. Ohashi, S. Ueda, H. Yoshikawa, Y. Yamashita, H. Oohashi and K. Kobayashi: Chem. Mater. **20** (2008) 4156–4160.
13) J. Gong, L. L. Wang, Y. Liu, J. H. Yang and Z. G. Zong: J. Alloy. Compd. **457** (2008) 6–9.
14) W. Zhou, K. Zheng, L. He, R. Wang, L. Guo, C. Chen, X. Han and Z. Zhang: Nano Lett. **8** (2008) 1147–1152.
15) S. Mourdikoudis, K. Simeonidis, A. Vilalta-Clemente, F. Tuna, I. Tsiaoussis, M. Angelakeris, C. Dendrinou-Samara and O. Kalogirou: J. Magn. Magn. Mater. **321** (2009) 2723–2728.
16) C. Chen, L. He, Y. Leng and X. Li: J. Appl. Phys. **105** (2009) 123923.
17) L. He: J. Magn. Magn. Mater. **322** (2010) 1991–1993.
18) S. C. Davis, S. J. Severson and K. J. Klabunde: J. Am. Chem. Soc. **103** (1981) 3024–3029.
19) P. Hooker, B. J. Tan, K. J. Klabunde and S. Suib: Chem. Mater. **3** (1991) 947–952.
20) L. Yue, R. Sabiryanov, E. M. Kirkpatrick and D. L. Leslie-Pelecky: Phys. Rev. B **62** (2000) 8969–8975.
21) Y. Leng, Y. Liu, X. Song and X. Li: J. Nanosci. Nanotechnol. **8** (2008) 4477–4481.
22) B. Ghosh, H. Dutta and S. K. Pradhan: J. Alloy. Compd. **479** (2009) 193–200.
23) Z. L. Schaefer, K. M. Weeber, R. Misra, P. Schiffer and R. E. Schaak: Chem. Mater. **23** (2011) 2475–2480.
24) S. Nagakura: J. Phys. Soc. Jpn. **12** (1957) 482–494.
25) S. Nagakura: J. Phys. Soc. Jpn. **13** (1958) 1005–1014.